Reducing the impedance of the Travelling Wave Cavities Feed-forward and one turn delay feed-back

P. Baudrenghien, G. Lambert
CERN, Geneva, Switzerland

Abstract

As part of the effort to reduce the impedance seen by the beam, each of the four SPS 200 MHz Travelling Wave Cavities will be equipped with a dedicated feed-forward and one turn feed-back pair. The feed-forward is designed to reduce the transient beam loading induced by the entrance of the head of the proton batch in the cavity and lasting for the cavity filling time (620 ns). It uses as input the beam current measured by a longitudinal broad-band pick-up and produces an output that is added to the desired drive (creating the accelerating voltage) to the power amplifiers. The one-turn feed-back is a loop that reduces the modulation of the cavity voltage caused by the periodic passage of the batch at every turn. The two systems are presented with an emphasis on the theoretically achievable impedance reduction.

1 THE 200 MHZ TRAVELLING WAVE CAVITIES

In the SPS, protons are accelerated by four cavities of the travelling wave structure type [1]. They are 15.7 m long waveguides loaded with stems and drift tubes and terminated into a matched load. The RF power generator launches a wave that propagates along the axis in the same direction as the particle[1].

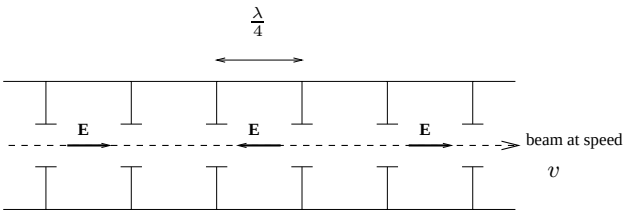

Figure 1: Principle of Travelling Wave acceleration.

At the centre frequency (200.222 MHz) the phase velocity of the wave is equal to the particle velocity v thereby resulting in the maximum effective accelerating voltage. When deviating from this frequency, phase velocity and particle velocity are different so that the particle slips with respect to the wave while crossing the cavity . This reduces the effective acceleration voltage[2]. The total phase slip τ is

$$\tau = \frac{L}{v_g}\left(1 - \frac{v_g}{v}\right) \times \Delta\omega \qquad (1)$$

where $\Delta\omega = \omega - \omega_0$ and ω_0 is the centre angular frequency[1]. In the above formula the ratio $\frac{v_g}{v}$ should be taken as negative because the structure is of the backward wave type. A generator current I_g will create an effective accelerating voltage V_{rf}:

$$V_{rf} = e^{j\phi_s} \times L\sqrt{\frac{Z_0 R_2}{2}} \times \left(\frac{\sin \tau/2}{\tau/2}\right) I_g = e^{j\phi_s} \times Z_{rf} \times I_g \qquad (2)$$

with ϕ_s the stable phase angle and Z_0 the characteristic impedance of the RF chain (50Ω). The above equation defines the forward transfer impedance Z_{rf}:

$$Z_{rf} = L\sqrt{\frac{Z_0 R_2}{2}} \times \left(\frac{\sin \tau/2}{\tau/2}\right) \qquad (3)$$

The cavity response is that of a pass-band centred at 200.222 MHz. It is plotted in figure 2. It is real valued and goes to zero when the frequency deviation produces a phase slip multiple of 2π (1.61 MHz, 3.23 MHz, 4.84 MHz,...). Notice the sign reversal at the zero crossing. The corresponding impulse response (Inverse Fourier Transform) is a rectangle lasting for 620 ns (and modulated at 200.222 MHz).

A beam current I_b travelling along the cavity axis will energize each individual cell (figure 1). The energy will then flow from one cell to the next. By integrating the induced electric field along the particle path, we get the volt-

Table 1: Parameters of the Travelling Wave Cavities (4 sections).

Centre frequency	200.222 MHz
Operating mode	$\pi/2$
Cell length	374 mm
Interaction length L (43 cells)	15.708 m
Group velocity v_g	$0.0946c$
Series impedance R_2	27.1 kΩ/m^2
Beam loading impedance $\frac{L^2 R_2}{8}$	0.84 MΩ

[1]The cavities are of the backward wave type: The group velocity v_g of the wave is opposite to the particle velocity v, but the phase velocity of the accelerating space harmonic is in the direction of v.

[2]The variation of the particle velocity with energy can be neglected.

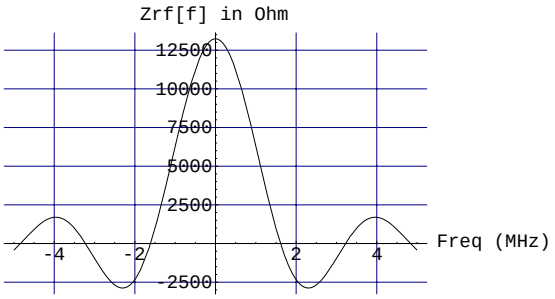

Figure 2: Forward transfer impedance Z_{rf} as a function of deviation from the centre frequency 200.222 MHz.

age seen by the beam V_b [1] [2]:

$$V_b = -\frac{L^2 R_2}{8}\left[\left(\frac{\sin\tau/2}{\tau/2}\right)^2 - 2j\left(\frac{\tau-\sin\tau}{\tau^2}\right)\right] I_b = Z_b \times I_b \quad (4)$$

This defines the beam transfer impedance Z_b:

$$Z_b = -\frac{L^2 R_2}{8}\left[\left(\frac{\sin\tau/2}{\tau/2}\right)^2 - 2j\left(\frac{\tau-\sin\tau}{\tau^2}\right)\right] \quad (5)$$

Z_b is plotted on figure 3. It has both a real and an imag-

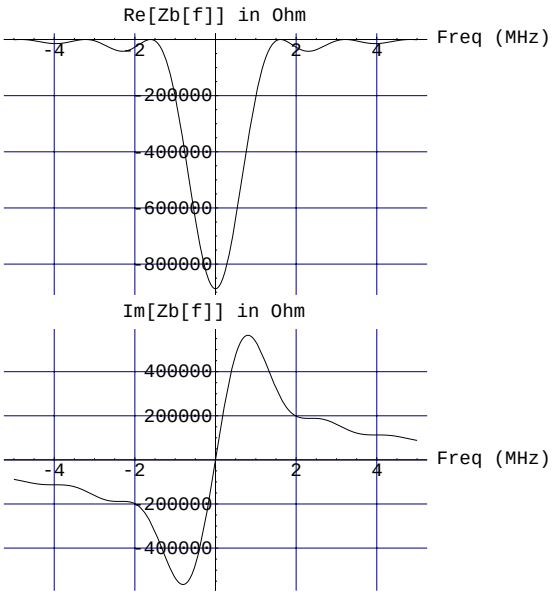

Figure 3: Beam transfer impedance Z_b as a function of deviation from centre frequency 200.222 MHz. (Top = real part, bottom = imaginary part).

inary part. Within a scaling factor, the real part is the square of the forward transfer impedance Z_{rf} (figure 2). But the imaginary part is completely different. Notice that it is non zero at the frequencies where Z_{rf} vanishes. Forward transfer impedance and beam loading impedance are identical for standing wave cavities. In our case they are completely different and this makes compensation of beam loading more difficult.

The first effect of Z_b is transient beam loading. The LHC beam in the SPS consists of one (or three) batches of 81 bunches spaced by 25 ns [3], [4]. The revolution period is $23\mu s$ (revolution frequency f_{rev} around 43kHz). When the head of the first batch enters into the cavity the beam loading voltage rises during 620 ns until it reaches its steady state value. This is the step response of the beam transfer impedance and it is exactly parabolic [5]. This voltage adds vectorially to the RF voltage in the cavity V_{rf}. Figure 4 shows the I (in phase) and Q (in quadrature) components of the beam loading demodulated with an arbitrary reference at the RF frequency. The bottom trace shows

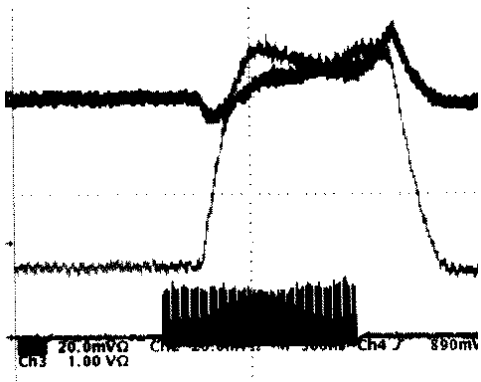

Figure 4: Transient beam loading at injection (first turn). 500ns per div.

the beam signal observed with a broad-band pick-up (one batch lasting for $2\mu s$). The total voltage seen by the beam varies from bunch to bunch in the head of the batch. The stable phase error at injection into the SPS excites bunch oscillations and after filamentation the longitudinal emittance of these bunches will be increased. (The phase loop of the beam control system adjusts the phase for the core of the batch only [6]). Transient beam loading is also a problem at transfer to the LHC: At 450 GeV the distance between SPS bunches would not be an exact multiple of the LHC RF frequency in the head of the batch. This implies a more demanding operation of the LHC longitudinal feedback system [7](large bandwidth). With a nominal intensity of 1.05×10^{11} protons per bunch, the 200 MHz component of the beam current I_b is 1.33 A for short bunches. The resulting beam loading voltage summed over the four cavities is then $V_b = 4.5$ MV. This value is very large compared to the 2 MV capture voltage V_{rf} at injection [6], [8] and the transient beam loading must be compensated. This will be achieved by reducing the apparent impedance at the frequencies $f_{RF} \pm n f_{rev}$.

The large beam loading impedance is also the cause of beam instabilities. This effect was first observed with the Fixed Target proton beam in 1979 [9]. Strong dipole oscillations were excited with mode number $n = 12$ or $n = 13$ (synchrotron sidebands of $f_{RF} \pm n f_{rev}$). To stabilize the

beam we must reduce the apparent impedance on the synchrotron sidebands of the revolution frequency lines (frequencies $f_{RF} \pm n f_{rev} \pm m f_s$) with f_s the synchrotron frequency. $m = \pm 1$ for the dipole mode and $m = \pm 2$ for the quadrupole mode. Figure 5 shows the envelope of the bunch current along the $2\mu s$ batch. The vertical scale is in thousands of turns. The first trace (bottom) shows the situation at injection: Constant bunch intensity along the batch. After 50 ms (2500 turns) a modulation develops near the tail of the batch and grows with time. The top trace is 100 ms after injection. The modulation is around 1.2 MHz. Its cause is the beam loading in the cavity and the loss of particle may be due to dipole oscillations.

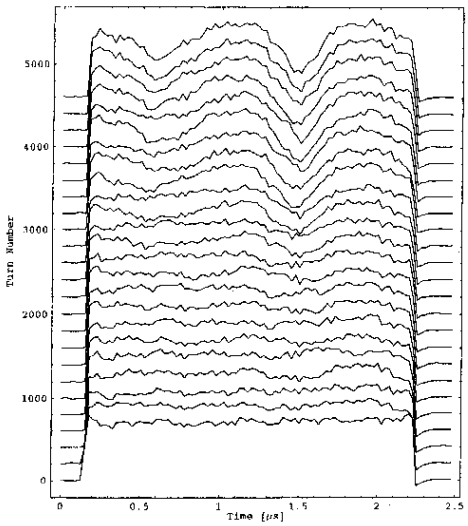

Figure 5: Instability at injection (0.5×10^{11} protons per bunch in one batch of 81 bunches). Each trace shows the envelope of the bunch intensity along the batch. Traces are separated vertically by 200 turns. 550kV capture voltage.

2 FEED-FORWARD CORRECTION

The total voltage seen by the beam is the sum of the voltage created by the generator and the beam loading:

$$V_t = V_{rf} + V_b = Z_{rf} I_g + Z_b I_b \qquad (6)$$

Figure 6 shows the feed-forward system: The beam current I_b is measured with a pick-up whose bandwidth should cover at least several tens of MHz around 200 MHz. It is then filtered by the transfer function H_{fwd} and the output is subtracted from the drive of the generator. The goal is to produce a correcting drive that compensates for the beam loading in the cavity. The filter must implement a band-pass around the centre frequency. This is realized by a frequency conversion system (figure 7): The input signal around 200 MHz is first translated into two baseband signals by two quadrature mixers (I and Q signals). These two signals are fed into identical digital filters operating at 20 MHz clock frequency. The outputs are then mixed up to the

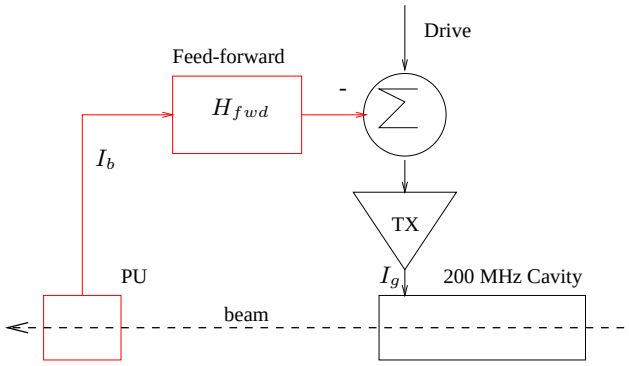

Figure 6: Principle of feed-forward correction.

passband. The transfer function H_{opt} is designed to minimize V_t in presence of beam loading: $H_{opt} Z_{rf} \approx Z_b$. The naive solution $H_{opt} = \frac{Z_b}{Z_{rf}}$ will not work however because Z_{rf} vanishes at frequencies where Z_b is non zero. Let us decompose H_{opt} into a real and an imaginary part:

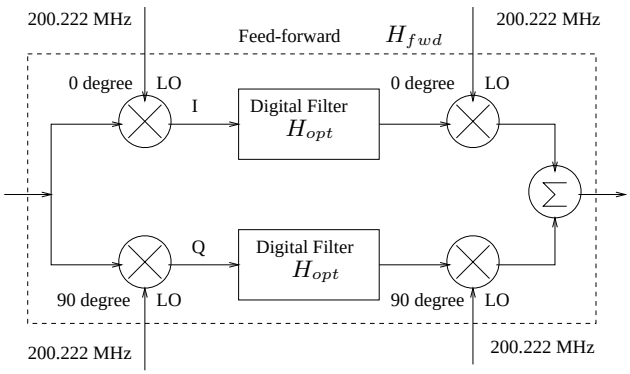

Figure 7: Band-pass filtering by downheterodyning, filtering in baseband and mixing up.

$$H_{opt} = H_{opt}^{re} + j H_{opt}^{im} \qquad (7)$$

Since Z_{rf} is real valued, our design goal is:

$$H_{opt}^{re} Z_{rf} + j H_{opt}^{im} Z_{rf} \approx Re[Z_b] + j Im[Z_b] \qquad (8)$$

By inspection of Z_{rf} (equation 3) and Z_b (equation 5) it follows that the real parts on the two sides can be made identical:

$$H_{opt}^{re} = -\frac{L}{4}\sqrt{\frac{R_2}{2Z_0}} \times \left(\frac{\sin \tau/2}{\tau/2}\right) \qquad (9)$$

and the compensation of the resistive part of beam loading is complete. The impulse response of H_{opt}^{re} is rectangular lasting for 12 samples at 20 MHz[3]. It is implemented with a Finite Impulse Response filter (FIR).

[3]The 620 ns long rectangle corresponds to 12.4 clock periods at 20 MHz, rounded to 12.

H_{opt}^{im} is also implemented with a FIR filter. Its impulse response h_n^{im} is limited to 31 samples ($-15 \leq n \leq 15$) and must be odd-symetric ($h_{-n}^{im} = -h_n^{im}$) so that its frequency response is purely imaginary. To proceed with the design we must choose a criterion for computing the optimal coefficients $h_1^{im}, h_2^{im}, ..., h_{15}^{im}$. We use the Least Squares Solution: Let a unit step current I_b enter the cavity (head of the batch) and consider the transient beam loading due to the difference between Z_b and the compensation $H_{opt} Z_{rf}$. This transient now lasts for 31 samples (H_{opt}) plus 12 samples (cavity response Z_{rf} lasting for 620 ns) equal 43 samples. The power of this transient (sum of the voltage squared over the 43 time samples) is a quadratic function of the 15 coefficients $h_1^{im}, h_2^{im}, ..., h_{15}^{im}$. Minimization of this power calls for the solution of a system of 15 linear equations with 15 unknowns. This easily gives the H_{opt}^{im}.

Figure 8 shows the theoretical performance of H_{opt}. The smooth parabolic curve is the actual beam loading voltage (downheterodyned) whose transient lasts for 12 time samples (from 22 to 33). The other curve shows the correction. The error is less than 5 percent. Notice the period of the error bumps (12 samples = 600 ns). It corresponds to the zeros of the forward transfer impedance (1.61 MHz and its harmonics).

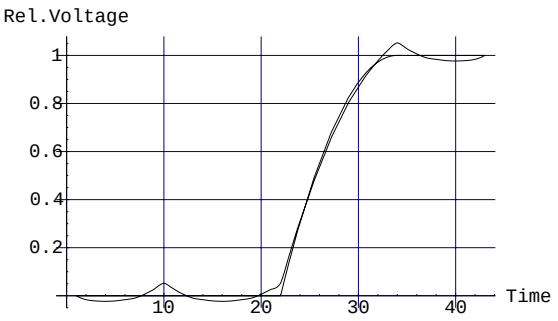

Figure 8: Theoretical performance of the feed-forward correction. Response to the head of the batch. Time scale in samples at 20 MHz.

In practice several factors limit the performance: A drift of the RF power generator gain by 1 dB will degrade a perfect compensation to 90 percent correction. The phase of the correction must be carefully adjusted at 200 MHz so that it aligns vectorially with the beam loading. It is difficult to maintain a long term accuracy to better than 10 degree because the RF frequency varies during the acceleration ramp (from 200.265 MHz to 200.395 MHz). This tolerance introduces an error of 17 percent in the compensation. At high frequencies the limiting factor is the reduced bandwidth of the power generators. Amplification is realized in a chain of four narrow-band stages [10]: The first two stages are double-tuned amplifiers[4]. Their single-sided -3 dB bandwidth is 4 MHz. They are followed by two single-tuned amplifiers[5] (2 MHz single-sided -3 dB bandwidth). The overall response has a single-sided -3 dB bandwidth of 1.5 MHz and the gain is reduced by 20 dB at 5 MHz from the centre. Figure 9 shows the I and Q components of the remaining beam loading. The situation is identical to the one of figure 4 but now the feed-forward is operating. Transient beam loading is reduced by a factor of 4 to 5 linear. The impedance reduction can be derived

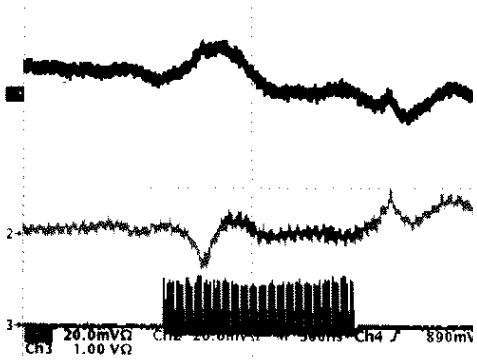

Figure 9: Remaining beam loading at injection (second turn) with feed-forward correction. Compare to figure 4 (without correction). 500ns per div.

from the remaining voltage in the cavity:

$$V_{uncorrected} = [Z_b - Z_{rf} H_{opt}]\, I_b \qquad (10)$$

and the impedance reduction $\Gamma_{feedfwd}$:

$$\Gamma_{feedfwd} = \left| \frac{Z_b - Z_{rf} H_{opt}}{Z_b} \right| \qquad (11)$$

The impedance reduction is plotted on figure 10. The power generators are modelled as the chain of tuned circuits described above. We can achieve 15 dB impedance reduction up to 1 MHz.

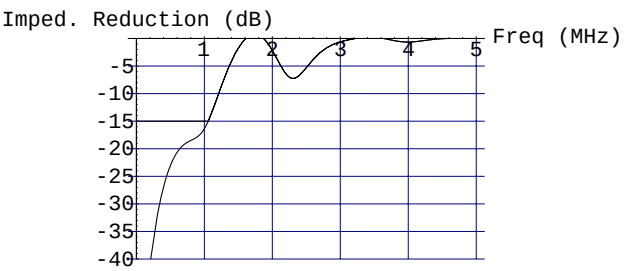

Figure 10: Computed impedance reduction with feed-forward correction. Reduction below -15 dB is unrealistic (equipment drifts).

3 FEED-BACK

Further compensation can be achieved by an RF feed-back (figure 11). The voltage sensed by the beam in each cell of

[4] Double-tuned amplifiers have two tuned circuits resonant to the same frequency with a coupling close to the critical value [11].

[5] Single-tuned amplifiers have only one resonant circuit.

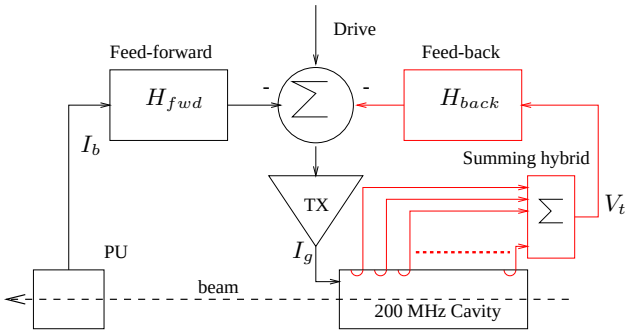

Figure 11: Beam loading correction by a feed-forward and feed-back pair.

the cavity (figure 1) is measured with a loop and delayed by the corresponding time of flight of the particle (i.e. a different delay for each loop). After addition of these signals in the summing hybrid we get the voltage seen by the beam V_t. This signal is filtered by the feed-back transfer function H_{back} and reinjected into the cavity with the proper phase via the power generator. The SPS cavities were equipped with RF feedback in 1983 [12]. The system presented here is an upgrade of the original design. The transfer function H_{back} implements a band-pass around 200 MHz. It is a heterodyne system similar to figure 7 but the Local Oscillator (LO) reference for the mixers is the RF frequency and the I and Q signals are AC coupled to the digital filters so that the feedback does not try to cancel the desired accelerating RF voltage V_{rf} [12]. The design of the digital filters H_{opt} will now be presented: The power generators are located in a surface building and connected to the cavity via a long coaxial line introducing a delay of $2.3\mu s$. We use the Long Delay Feedback method [2]: The digital filter H_{comb} has a large gain only in the vicinity of the revolution frequency harmonics $\pm n f_{rev}$ and the total delay in the loop is extended to exactly one revolution period so that the phase shift is zero where the gain is maximum (figure 12). The z-transform of the filter is:

$$H_{comb}(z) = \left(\frac{1-a}{1-az^{-N}}\right) z^{-N} \qquad (12)$$

where N sampling periods equal one turn. The parameter a governs the bandwidth of the filter around each revolution frequency harmonic. We use a 40 MHz clock ($N = 924$) and 450 Hz single-sided bandwidth ($a = \frac{15}{16}$). The open-loop response of the feed-back includes the cavity response Z_{rf} reconstructed by the summing hybrid (figure 13). This leads to 180 degree phase jumps at 1.61 MHz, 3.23 MHz, 4.84 MHz, ...To maintain stability the feedback frequency response must also change sign at these frequencies. This is the role of the post-filter H_{pf}. It must have gain at the lower frequencies because Z_b is maximum there and its gain must increase with frequency to compensate for the decrease of the forward transfer impedance Z_{rf}. It is thus an all-pass with more gain at the higher frequencies. It consists of two branches in parallel (figure 14).

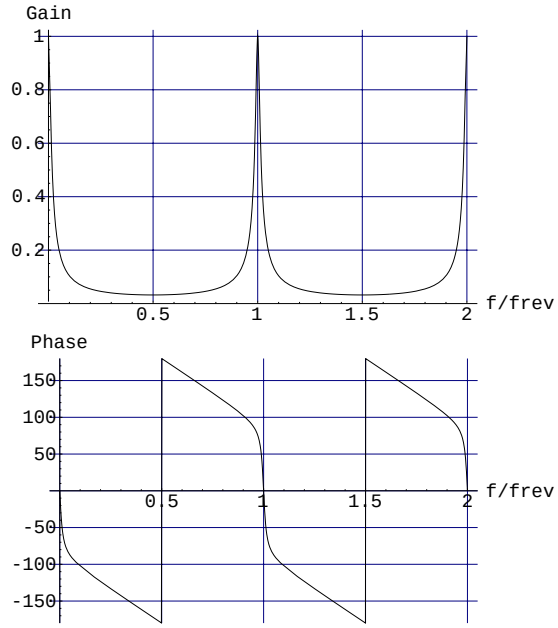

Figure 12: Gain and phase response of the digital comb filter H_{comb} ($a = \frac{15}{16}$).

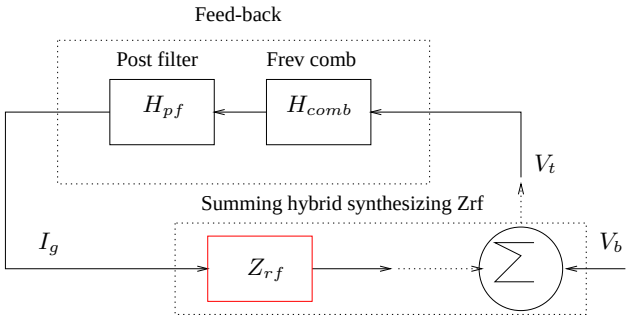

Figure 13: Feed-back loop including the cavity response Z_{rf}.

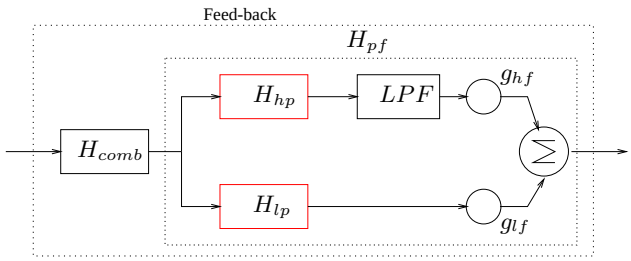

Figure 14: Feed-back showing the two branches of the post-filter: lower branch = low-pass, upper branch = high-pass.

The lower branch H_{lp} is a low-pass:

$$H_{lp}(z) = \frac{1}{M}\left(\frac{1-z^{-M}}{1-z^{-1}}\right) z^{\frac{M-1}{2}} \qquad (13)$$

We choose $M = 25$ so that, with a 40 MHz sampling frequency, H_{lp} has zero frequency response at 1.60 MHz, 3.20 MHz, 4.80 MHz,... and its sign changes there. Within a scaling factor its frequency response is identical to Z_{rf}. It is easily implemented with a FIR filter: Its impulse response is a rectangle lasting for 25 samples (625 ns). The upper branch H_{hp} is meant to extend the bandwidth:

$$H_{hp}(z) = -\frac{1-b}{4}\left(\frac{1-z^{-M}}{1-bz^{-M}}\right)\left(1-z^{-1}\right) z^{\frac{M+1}{2}} \qquad (14)$$

Its frequency response is plotted in figure 15 for $M = 25$ and $b = \frac{1}{2}$. Notice the 180 degree phase jumps at the desired frequencies. The gain increases continuously up to

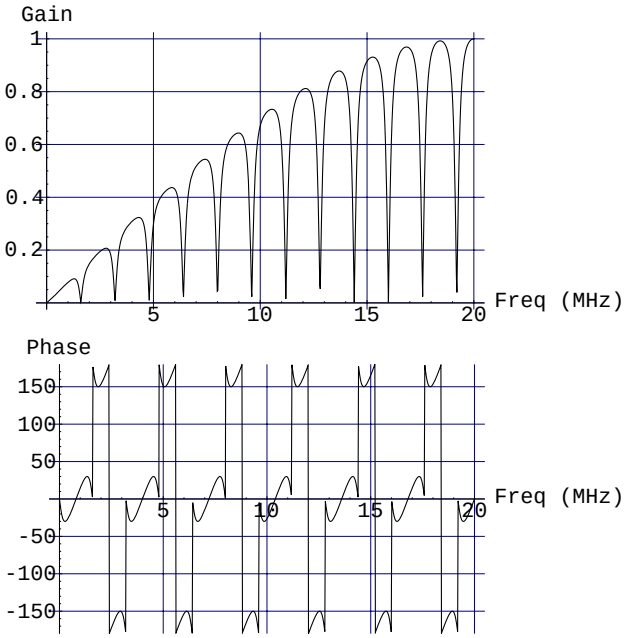

Figure 15: Gain and phase response of the high-pass filter H_{hp}.

half the sampling frequency. This is not desirable: It would inject high frequency noise into the power generator drive. Very fast transients may also trip the amplifiers. The high-pass filter is therefore followed by a low-pass filter (LPF in figure 14) that filters out the higher part of the spectrum (above 8 MHz, adjustable). It is implemented as an even-symetric FIR so that it does not introduce phase shift. (Its frequency response is real). Finally the signals from the two branches are added with adjustable gains g_{hf} and g_{lf}.

The impedance reduction $\Gamma_{feedback}$ achieved by the feed-back alone is:

$$\Gamma_{feedback} = \frac{1}{1 + H_{comb} H_{pf} Z_{rf}} \qquad (15)$$

Keeping a 10 dB gain margin and including the band-limited power generator, we obtain the impedance reduction shown in figure 16. The figure plots the enveloppe of the reduction: Actually the impedance is only reduced in the vicinity of the revolution frequency harmonics. The synchrotron frequency f_s varies between 100 Hz and 450 Hz during the acceleration cycle [6]. With $a = \frac{15}{16}$ the open loop gain (figure 12) has decreased by 3 dB on the first synchrotron side-bands in the worst case ($f_s = 450$Hz) and by only 0.2dB in the best case ($f_s = 100$Hz). The impedance reduction for the dipole mode is thus respectively about 3db and 0.2 dB less efficient than shown on figure 16. For the quadrupole mode $f_{RF} \pm n f_{rev} \pm 2 f_s$ it is respectively 7db and 0.7dB less efficient.

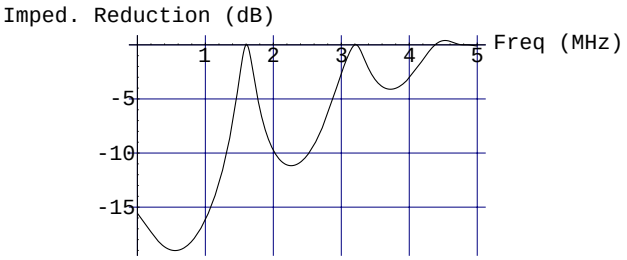

Figure 16: Computed impedance reduction with feed-back alone. ($g_{hp} = 30 g_{lp}$).

4 FEED-FORWARD AND FEED-BACK PAIR ON ONE CAVITY

For each cavity we have a pair of feed-forward and feed-back as shown on figure 11. The achieved impedance reduction is the product of $\Gamma_{feedfwd}$ and $\Gamma_{feedback}$. Figure 17 shows what can be achieved with the band-limited RF power generators: 30 dB impedance reduction up to 1 MHz. During the 1999 run one cavity was tested with a

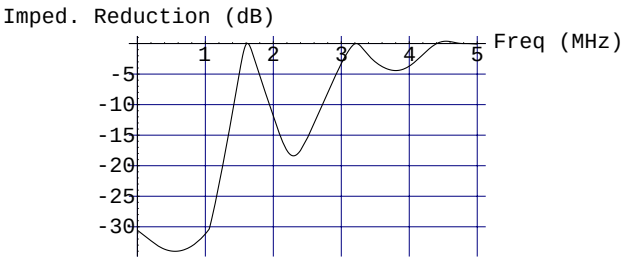

Figure 17: Computed impedance reduction with a feed-forward and feed-back pair.

feed-forward and a simplified feed-back missing the high-pass branch in the post-filter. The cavity under test consisted of five sections (54 interaction cells) instead of the four sections (43 cells) foreseen for the LHC era and the

filters were adapted to this length[6]. The beam loading compensation is illustrated in figure 18 showing also the performance of each system alone. The final compensation (figure at the bottom) shows a remaining high frequency transient at the head of the batch. It will hopefully be reduced with the upgraded feed-back (high-pass branch in the post-filter).

5 COUPLED FEED-BACK AROUND TWO CAVITIES OF DIFFERENT LENGTHS

The frequencies where impedance reduction is impossible are the zeros of Z_{rf}. Equations 1 and 3 indicate that they scale with the inverse of the cavity length. Figure 19 presents two feed-back coupled on two cavities of different lengths: A long cavity of 4 sections (zeros of the forward transfer impedance at 1.61 MHz and its harmonics) and a short cavity of 3 sections whose zeros are at 2.16 MHz and its harmonics. The input to the feed-back around each cavity is the sum of the voltages in the two cavities. The beam induced voltage at 1.61 MHz in the long cavity can be compensated by the feed-back in the short cavity and vice versa at 2.16 MHz. The achievable overall impedance reduction (without feed-forward) is shown in fig 20. The open loop gains are adjusted keeping the 10 dB gain margin. The transfer functions of the feed-back systems are as presented in equations 12, 13 and 14 and the parameter M is adjusted to the cavity length ($M = 18$ for the 32 cells cavity). Comparing figure 20 with figure 16 we see that impedance reduction is now achieved around the zeros of each cavity.

6 CONCLUSIONS

The problem of transient beam loading in the head of the batch is reduced significantly by the feed-forward and feed-back pair on each cavity (system shown on figure 11). The remaining emittance blow up due to stable phase error at injection is acceptable. In addition this system will ease the operation of the 200 MHz longitudinal damping system at transfer into the LHC.

The issue of potential beam instabilities is more complex: It is expected that the nominal LHC beam will remain stable if the impedance of the cavities is reduced by 20 dB up to 1 MHz [13]. If so, the system of figure 11 will be sufficient. To prepare the SPS as LHC injector all four cavities will be shortened to four sections, this being the optimium cavity length with beam loading for the ultimate current [4],[14]. The possibility exists that the beam becomes unstable at the exact notch frequency of these cavities where no compensation is possible (1.61 MHz). If this is observed, we can shorten one cavity to three sections and use a coupled feed-back system as shown in figure 19.

[6]The cavities are made of sections of eleven cells. One half of the two end cells do not participate to the acceleration.

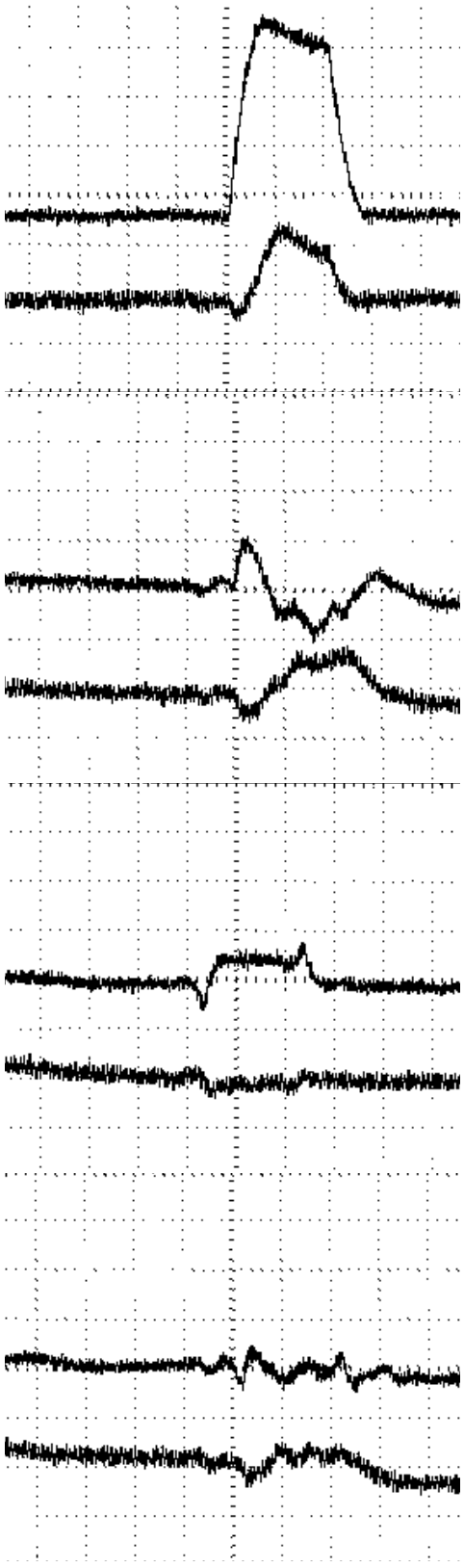

Figure 18: Beam loading compensation with the LHC batch of $2\mu s$ ($1\mu s$ per division). I and Q components of the beam loading. From top to bottom: no compensation, feed-forward only, feed-back only, feed-forward and feed-back pair. (5 sections cavity, feed-back with low-pass branch H_{lp} only).

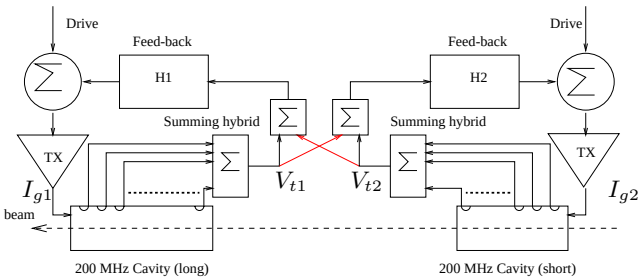

Figure 19: Coupled feed-back on two cavities of different lengths.

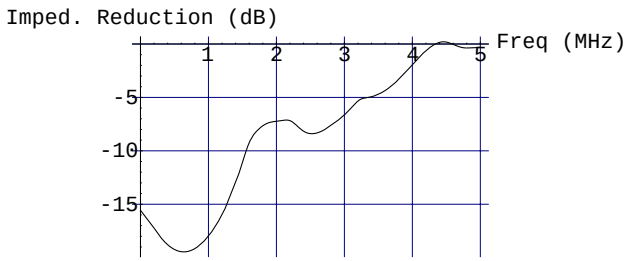

Figure 20: Computed overall impedance reduction with two cavities of different lengths (43 cells and 32 cells) coupled via their feed-back systems. (No feed-forward).

In the meantime the SPS is operated with two cavities of four sections and two cavities of five sections. For the start-up 2000 all four cavities will be equipped with a private feed-forward system. A prototype upgraded feed-back (integrating the high-pass branch) will be tested on one cavity during the spring 2000. If it performs well all four cavities will receive a feed-forward and feed-back pair before the end of the run 2000.

7 ACKNOWLEDGEMENTS

We wish to thank our colleagues in the SL/HRF/BC section and the SL operation crew for their help during the machine development sessions preparing the SPS for the LHC. We are also very grateful for the work done by R. Cappi, R. Garoby and D. Manglunki from the PS division to provide the LHC test beams.

8 REFERENCES

[1] G. Dôme, The SPS accelerating system, Travelling Wave Drift-Tube structure for the CERN SPS, CERN-SPS/ARF/77-11, May 77.

[2] D. Boussard, Beam loading, Cern Accelerator School, Oxford, England, 16-27 September 1985, CERN 87-03, 21 April 87.

[3] LHC, Conceptual Design, CERN/AC/95-05 LHC, 20 October 95.

[4] The SPS as Injector for LHC, Conceptual Design, CERN/SL/97-07 DI, 4 March 97.

[5] D. Boussard, Travelling-wave structures, Joint US-CERN-Japan Accelerator School on Frontiers of Accelerator Technology, Tsukuba, Japan , 9 - 18 Sep 1996, Published in:Proceedings S I Kurokawa, M Month and S Turner World Sci., Singapore, 1999.

[6] P. Baudrenghien, Beam Control for Protons and Ions, IX th LEP-SPS Performance Workshop Chamonix, France, 25-29 January 99, CERN-SL-99-007-DI.

[7] D. Boussard, E. Chiaveri, H.P. Kindermann, T. Linnecar, S. Marque, J. Tuckmantel, Design Considerations for the LHC 200 MHz System, LHC Project Report 368, January 2000.

[8] T. Linnecar, E. Shaposhnikova, Requirements for beam parameters in the SPS when used as LHC injector, SL Note/94-87(RF), October 94.

[9] D. Boussard, G. Dôme, T.P.R. Linnecar, Acceleration in the SPS, Present status and future developments, IEEE Transactions on Nuclear Science, Vol. NS-26, No. 3, June 1979.

[10] F. Oude Moleman, Private communication.

[11] F.E. Terman, Radio Engineering, McGraw-Hills Publishing, London 1951.

[12] D. Boussard, G. Lambert, Reduction of the apparent impedance of wide band accelerating cavities by RF feedback, IEEE Transactions on Nuclear Science, Vol. NS-30, No. 4, August 1983.

[13] T. Linnecar, Private communication.

[14] T. Bohl, Running RF with high beam loading, X th LEP-SPS Performance Workshop Chamonix, France, 17-21 January 00, these proceedings.